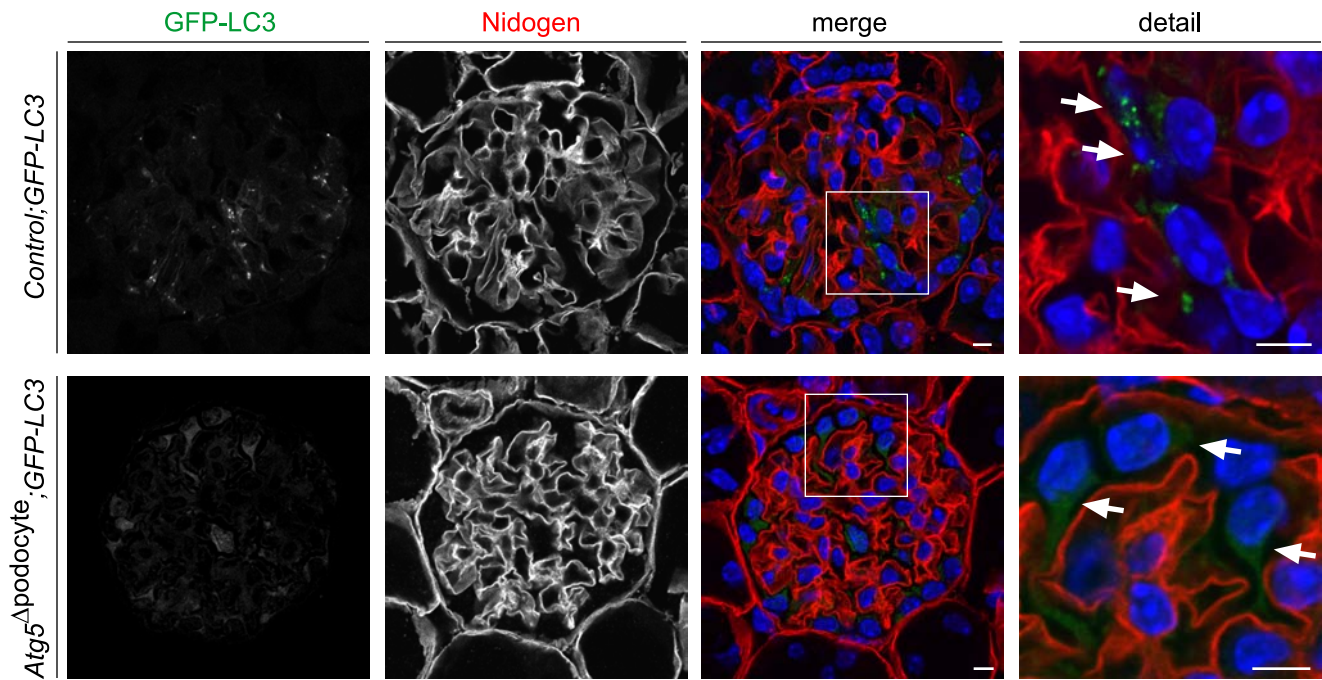


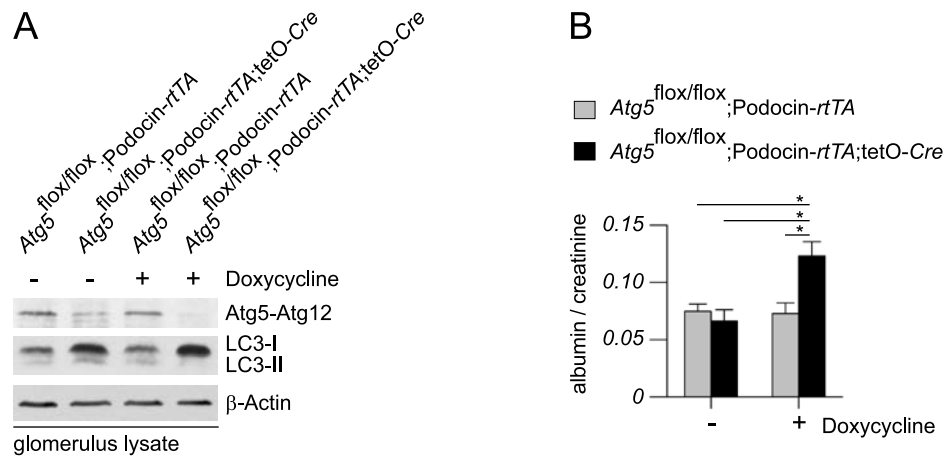
Supplemental Figure 1



Supplemental Fig. 1: Absence of GFP-LC3 positive vesicles in podocytes of *Atg5*^{Δpodocyte}; *GFP-LC3* mice.

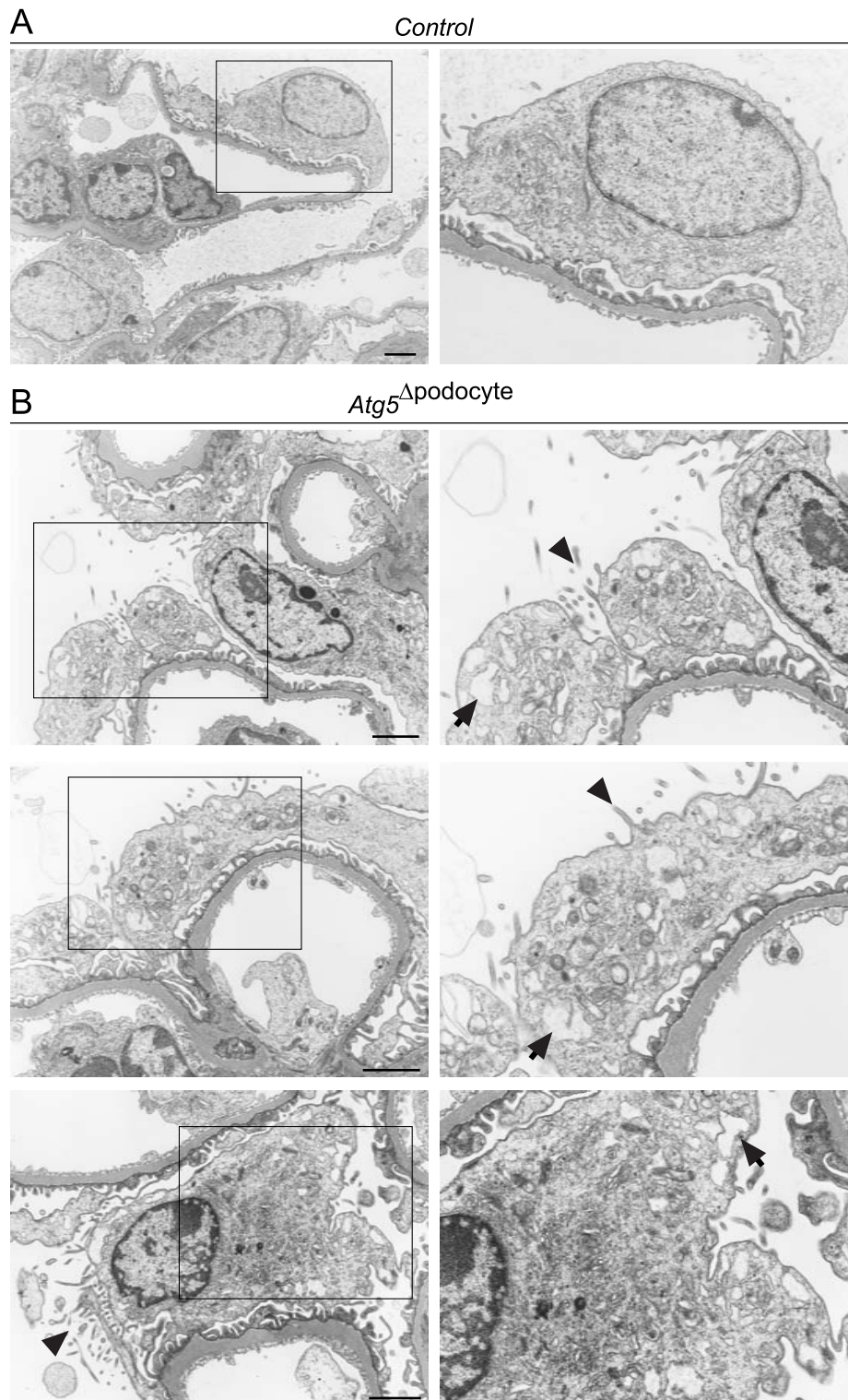
Podocyte-specific *Atg5* deficient mice (*Atg5*^{Δpodocyte}) were crossed to *GFP-LC3* transgenic mice to confirm the functional ablation of autophagy. In these triple transgenic mice glomerular GFP-LC3 positive vesicles were completely absent and GFP-LC3 was diffusely distributed in the cytoplasm, while GFP-positive autophagosomes could be detected in control *GFP-LC3* mice (arrows indicate GFP-LC3 positive autophagosomes in the control condition or cytosolic GFP-LC3 signal in the *Atg5* knockout condition respectively). Scale bars: 5 μ m.

Supplemental Figure 2



Supplemental Fig. 2: Doxycycline dependent induction of podocyte specific *Atg5* knockout. (A) *Atg5*-floxed mice (*Atg5*^{flox/flox}) were crossed with Podocin-rtTA;tetO-Cre to generate Doxycycline-inducible podocyte-specific *Atg5* knockout mice (*Atg5*^{flox/flox};Podocin-rtTA⁺;tetO-Cre⁺); tetO-Cre⁻ littermates served as control. Western blot analysis of isolated glomeruli from *Atg5*^{flox/flox};Podocin-rtTA⁺;tetO-Cre⁺ or *Atg5*^{flox/flox};Podocin-rtTA⁺ mice confirmed the absence of Atg5 after Doxycycline administration and displayed the abrogated conversion of LC3-I. (B) Induction podocyte-specific *Atg5* knockout in 12 weeks old mice resulted in a significant increased albuminuria (n=6 for each condition, *=two-tailed Student's t-test p<0.05).

Supplemental Figure 3

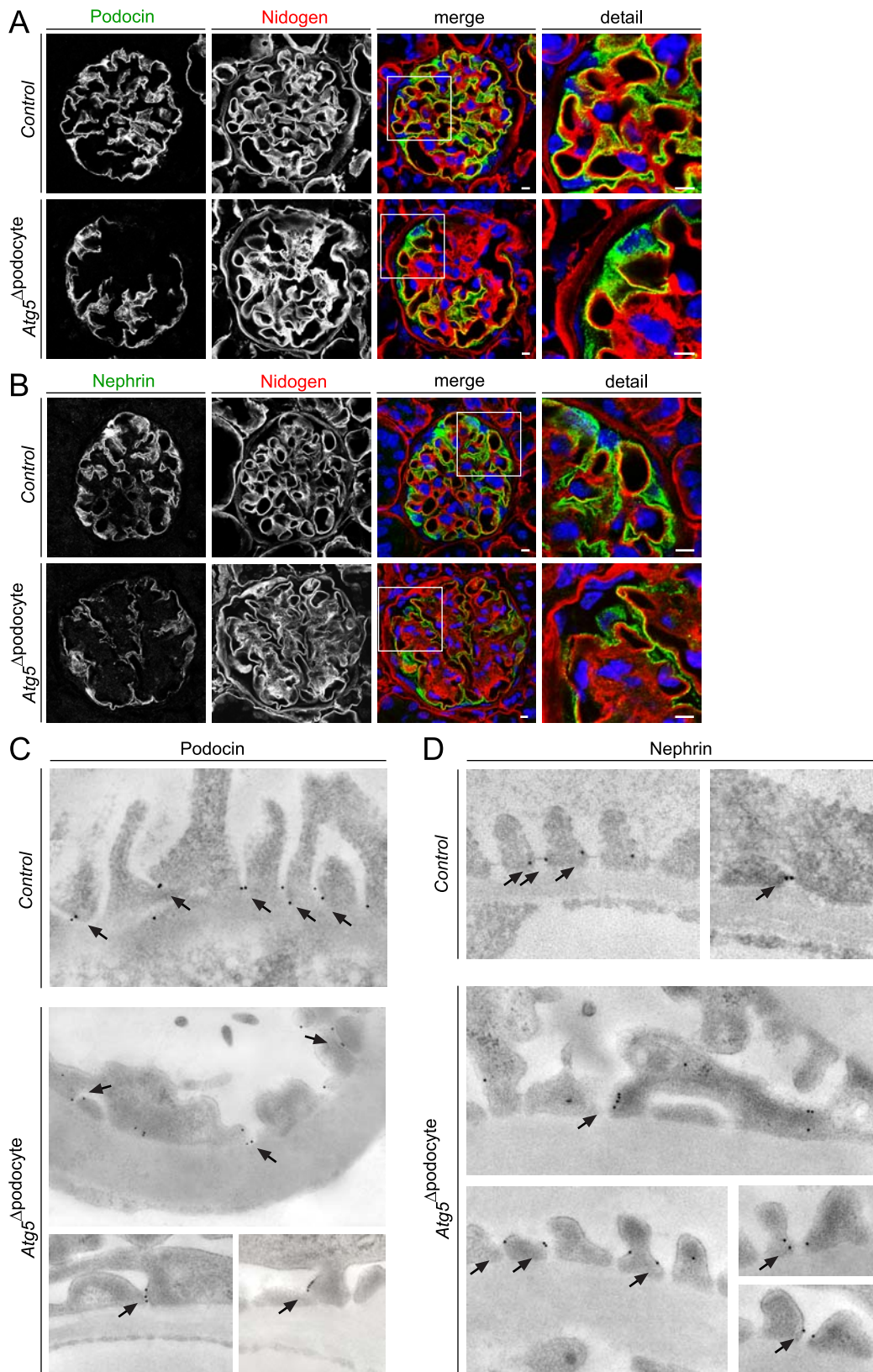


Supplemental Fig. 3: Detailed EM analysis of 12 month old *Atg5^Δpodocyte* mice with mild albuminuria.

(A) Control littermates showed normal podocyte morphology with a regular foot process network.

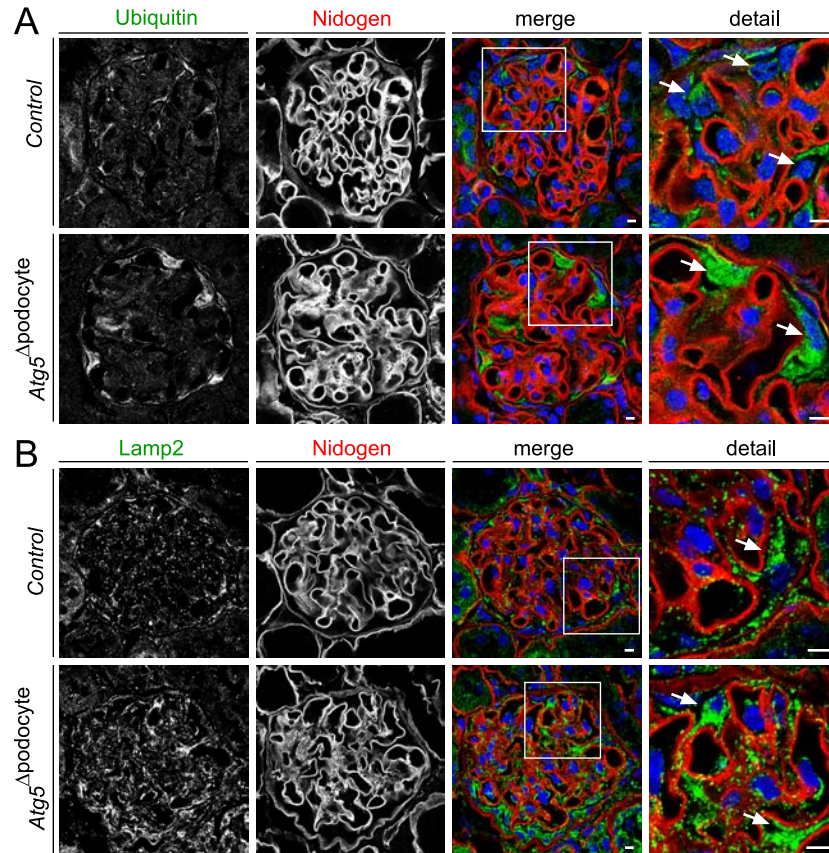
(B) *Atg5^Δpodocyte* mice displayed abnormalities such as cisternal distension of rough ER (arrows), aberrant membranous structures, and microvillus formation (arrowheads). Scale bars: 2 μ m.

Supplemental Figure 4



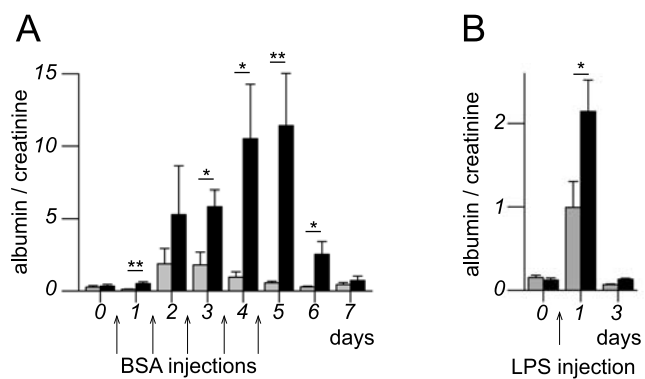
Supplemental Fig. 4: Slit diaphragm proteins in 22 month old *Atg5*^{Δpodocyte} mice. Immunofluorescence and specific immunogold stainings of the slit diaphragm proteins podocin (**A**, **C**) and nephrin (**B**, **D**) in non-sclerosed glomeruli of 22 month old *Atg5*^{Δpodocyte} and control mice. Nidogen served as basement membrane marker. Scale bars: 5 μ m. Arrows indicate gold particles.

Supplemental Figure 5



Supplemental Fig. 5: Protein degradative pathways in 22 month old *Atg5* Δ podocyte mice. Confocal microscopy of kidneys from *Atg5* Δ podocyte and control mice demonstrated an accumulation of ubiquitin positive aggregates (**A**) and Lamp2 positive structures (**B**) in *Atg5* Δ podocyte mice. Arrows indicate podocytes. Scale bars: 5 μ m.

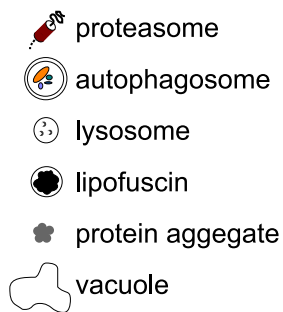
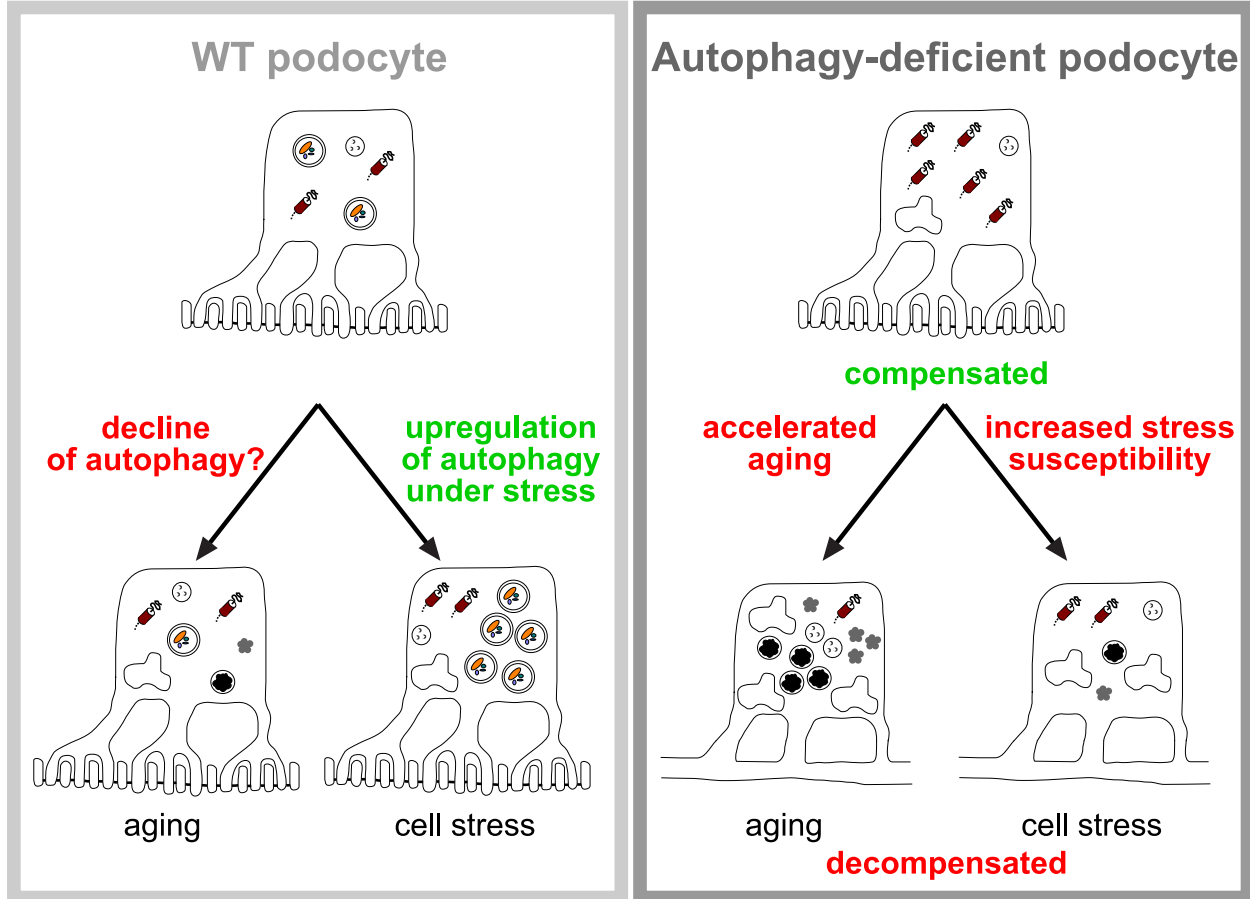
Supplemental Figure 6



Supplemental Fig. 6: Induction of albuminuria in the BSA overload model and LPS model.

Low doses of BSA (**A**) or LPS (**B**) respectively caused a significant higher transient albuminuria in *Atg5* Δ podocyte mice compared to control littermates (BSA n=6 for control- and n=5 *Atg5* Δ podocyte mice, LPS n=4 for control and *Atg5* Δ podocyte mice, * =two-tailed Student's t-test p<0.05).

Supplemental Figure 7



Supplemental Fig. 7: Autophagy controls podocyte aging, maintenance and glomerular disease susceptibility. Schematic illustration summarizing the role of autophagy for glomerular biology and glomerular disease: Autophagy is an important mechanism for podocyte homeostasis and maintenance, and a decline of autophagy might contribute to the age-related loss of glomerular function. Genetic deletion of autophagy in podocytes results in an accelerated podocyte aging and a dramatically increased susceptibility to glomerular stress. The autophagy-lysosome system and the UPS appear to be functionally coupled and *Atg5* deficient podocytes upregulate the proteasome activity to partially compensate for the loss of autophagy.